Japanese Journal of Applied Physics
Vol. 45, No. 10B, 2006, pp. 8457–8461

Effect of Indium-Oxide Deposited Using an Oxygen Ion-Beam-Assisted-Deposition to Top-Emitting Organic Light-Emitting Diodes

Chang Hyun JEONG, Jong Tae LIM, June Hee LEE, Mi Suk KIM, Jeong Woon BAE and Geun Young YEOM*

Department of Advanced Materials Science and Engineering, Sungkyunkwan University, Chunchun-Dong, Jangan-Gu, Suwon 440-746, Korea

(Received January 24, 2006; revised April 14, 2006; accepted June 18, 2006; published online October 24, 2006)

Indium oxide thin films have potential applications as cathodes in top-emitting organic light-emitting diodes (TEOLEDs). This study examined the characteristics of transparent conducting indium oxide (IO) films deposited by an oxygen ion-beam-assisted-deposition (IBAD) as a function of the applied oxygen ion energy (V_a). When TEOLED devices consisting of glass/Ag (100 nm)/ITO (125 nm)/2-TNATA (30 nm)/NPB (15 nm)/Alq_3 (55 nm)/LiF (1 nm)/Al (2 nm)/Au (20 nm)/IO (100 nm) were fabricated at a lower V_a, a lower turn-on voltage was observed even though the maximum luminance (32,000 cd/m^2) was similar one another. A V_a of approximately +50 V produced an IO film with a resistivity of 8.5×10^{-4} Ω·cm and a transmittance of 85%. The definition (I–V) characteristics of TEOLED devices with a cathode layer of Al (2 nm)/Au (20 nm)/IO (100 nm) were similar to the device fabricated with Al (2 nm)/Au (20 nm) only. [DOI: 10.1143/JJAP.45.8457]

KEYWORDS: IBAD, TEOLED, IO, buffer layer, Al/Au

1. Introduction

Organic light-emitting diode (OLED) devices have attracted considerable attention for potential applications in the next generation of flat panel displays on account of their high luminescence, high efficiency, wide color range, easy fabrication process, and potential for flexible displays.[1–3] In particular, top-emitting OLED (TEOLED) devices are being investigated intensively for use in active-matrix displays with a high aperture ratio due to their geometrical merit in allowing a high pixel resolution.[4,5] One of the factors determining the performance of TEOLED devices is the property of the top electrode consisting of only transparent conducting oxides (TCO) or a buffer layer/TCO.[6–10] Therefore, a high transmittance as well as a low resistance is essential for obtaining a better performance such as a high luminance and low turn-on voltage.

In the fabrication of TEOLED devices, electrode materials consisting of metal and TCO are generally deposited by evaporation or dc/rf sputtering techniques, which are widely used in semiconductor processing.[4,5,11] In particular, dc or rf sputtering are commonly used in the cathode deposition of OLEDs. Organic materials in OLED devices are easily damaged. Therefore, transparent or semi-transparent conducting buffer layers are deposited on the device, prior to depositing the TCO layer in order to reduce the damage by the species in the plasma during the deposition of TCO layer. Even though the addition of such buffer layers can reduce the level of damage during TCO deposition, it is difficult to avoid damage to the organic layer because of the high sensitivity of organic films to radiation, charging, heat, oxidation, etc. In particular, during conventional sputter deposition processing, energetic particles such as reflected neutrals, high-energy γ electrons, and charged ions can attack the surface of the organic layers and transfer their high energies to the organic layers. In addition, the organic layers can be oxidized by oxygen atoms and ions during the oxide sputter deposition.[12] These degrade the underlying organic layers and/or a buffer layer such as Al.

One of the techniques for depositing TCO films is oxygen ion-beam-assisted-deposition (IBAD). IBAD operates at a higher vacuum than used in sputtering techniques and the oxygen ion bombardment energy can be varied, which reduces the damage occurring during the deposition of TCO. Therefore, low-energy oxygen IBAD was used to deposit TCO in order to reduce the level of damage to the organic layer and buffer layers while fabricating the electrodes on the organic layers of a OLED device. This study examined the optical and electrical properties of the TCO thin films deposited at low energy, as well as the electrical and luminance characteristics of the TEOLED devices fabricated with the TCO as the cathode material.

2. Experimental Methods

Figure 1(a) gives a schematic device configuration of TEOLED, which consists of glass/Ag (100 nm)/ITO (about 20–30 Ω/□)/2-TNATA (30 nm)/NPB (15 nm)/Alq_3 (55 nm)/LiF (1 nm)/Al (2 nm)/Au (20 nm)/IO (100 nm). In detail, the structure of the TEOLED consisted of a multilayer anode of Ag/ITO, an organic multilayer of 2-TNATA/NPB/Alq_3, LiF, and a multilayer cathode Al/Au/ITO, respectively. First, the 100-nm-thick Ag layer consisting of the multilayer anode was vacuum-evaporated using an electron beam evaporator. A 125-nm-thick tin-doped indium (ITO) layer was deposited onto this Ag layer by dc sputtering, which is carried out at a pressure of 5 mTorr in argon mixed with <2% oxygen and a dc power of 400 W. An edge-passivation layer of the 200-nm-thick SiO_2 was then deposited onto the ITO layer using an electron beam evaporator to prevent a short-circuit between the top cathode and bottom anode layers during TCO deposition. Second, organic layers consisting of 30-nm-thick 2-TNATA, 15-nm-thick NPB, 55-nm-thick Alq_3 and lithium fluoride (LiF) as an electron-transporting layer (EIL) were deposited sequentially using a thermal evaporator. Finally, 2-nm-thick Al and 20-nm-thick Au layers consisting of the multilayer cathode was deposited onto LiF using a thermal evaporator, and a capping ITO layer was deposited by dc sputtering, which was carried out at a pressure of 5 mTorr in argon mixed with O_2 controlled by a MFC and an attached a needle valve at dc power of 100 W.

*Corresponding author. E-mail address: gyyeom@skku.edu

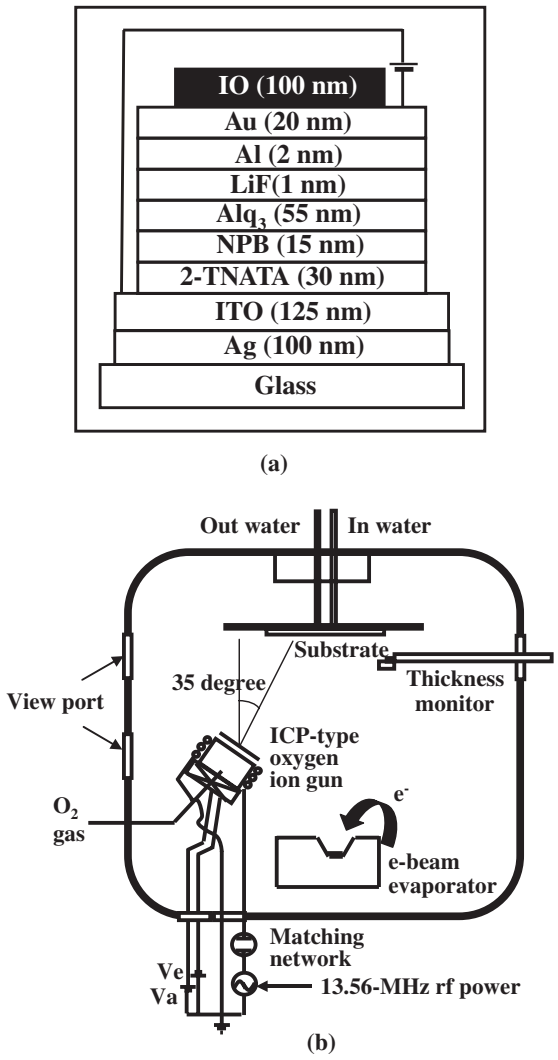

Fig. 1. (a) Schematic device configuration of the TEOLEDs fabricated. (b) The schematic diagram of the oxygen IBAD system used in the experiments.

Among the organic layers, 4,4′,4″-tris[2-naphthylphenyl-1-phenylamino]triphenylamine (2-TNATA) and 4,4′-bis[*N*-(1-napthyl)-*N*-phenyl-amino]-biphenyl (NPB) were used as a hole-injecting layer (HIL) and as a hole-transporting layer (HTL), respectively. In addition, tris(8-quinolinolato) aluminum(III) (Alq_3) was used as both a green emissive material layer (EML) and an electron-transporting layer (ETL). In the layers for the TEOLED devices, aluminum (2 nm)/Au (20 nm) was used as a buffer cathode layer to reduce the amount of damage to the organic layers and prevent oxidation of the electrode during IO deposition. The emissive active area of the devices was $2 \times 2\,mm^2$.

IO thin film deposition was carried out using an IBAD system. Figure 1(b) gives a schematic diagram of the deposition system used in this study. The ion gun of the IBAD system faced the substrate holder at an angle of 35° to the surface normal of the substrate in order to decrease the level of physical damage to the substrate. The IBAD system consisted of both an electron beam evaporator as the source of the IO flux and plasma ion gun as the oxygen ion beam source. The ion gun was driven by an rf inductively coupled plasma of 13.56 MHz. The ion gun consisted of two grids that were used to efficiently extract and accelerate the generated ions. The 1st grid to extract oxygen ions was located at the front of the ion gun source. The 2nd grid used to accelerate oxygen ions was located at the rear, as shown in Fig. 1(b).

The ion gun was operated at a rf power of 300 W and an extraction voltage (V_e) of −100 V, and by varying V_a from +50 to +300 V, the oxygen ion energy to the substrate was changed. The oxygen gas flow rate to the ion gun was maintained at 18 sccm. The deposition rates of IO using oxygen IBAD were varied from 0.10 to 0.16 nm/s. The source for the electron beam evaporation of IO was a pellet of IO with a 99.99% purity (PURE TECH).

The reflectance spectrum of the glass/Ag/ITO anode and transmittance spectrum of both the Al/Au and IO cathode layer were measured using a definition (UV–vis–NIR) spectrophotometer with an attached VW specular wavelength reflectance (Varian, Cary 5000 UV/VIS/NIR). The resistivity was measured using a four-point probe (CHANG MIN, CMT-SERIES). The electrical characteristics of the fabricated TEOLED devices were measured using a Keithley 2400 electrometer, and the luminance characteristics of the TEOLED devices were observed using a photodiode (oriel 71608) and Keithley 485 picoammeter. The electroluminescent (EL) spectra of the fabricated devices were obtained using optical emission spectroscopy (OES; SC Tech., PCM-420).

3. Results and Discussion

The device structure of the TEOLED examined in this study consisted of glass/Ag (100 nm)/ITO (125 nm)/2-TNATA (30 nm)/NPB (15 nm)/Alq_3 (55 nm)/LiF (1 nm)/Al (2 nm)/Au (20 nm)/IO (100 nm). Among these layers, a protective buffer layer of Al (2 nm)/Au (20 nm) was used to protect the organic layers from the energetic particles, electrical charging, heat, light, etc., and prevent the oxidation of the electrode that can occur during IO deposition by IBAD. A cathode material, which has a similar work function as that of Alq_3, is required for the effective electron injection from the cathode to Alq_3 layer. Hung *et al.* reported effective electron injection to the Alq_3 layer using LiF/Al bi-layer with the Al thickness of approximately 0.1 nm.[13] In addition, instead of LiF/Al only, a buffer layer consisting of a LiF/Al/Ag layer are widely used to reduce the level of damage or oxidation during the deposition of the following TCO layer. However, Ag can be also easily oxidized by oxygen and water, and has high reflectance/low transmittance, which is undesirable for the characteristics of the cathode layer for TEOLED devices. Therefore, this study used LiF/Al/Au as the cathode buffer layer instead of LiF/Al/Ag, because it has higher transmittance and oxidation resistance.

A 100-nm-thick IO layer was deposited on the top of the LiF (1 nm)/Al (2 nm)/Au (20 nm) using oxygen IBAD while changing the oxygen ion energy from +50 to +300 V by varying V_a. The extraction grid voltage, oxygen to the ion gun and rf power to the ion gun was maintained at −100 V, 18 sccm, and 300 W, respectively. Due to the differences in the oxygen flux at different oxygen ion gun energies, the e-beam evaporation of IO was varied and optimized. Actually, there will be small change in the oxygen ion beam flux arriving at the substrate as the acceleration energy of the

Table I. The deposition rate and electrical resistivity of the IO thin film when the oxygen ion gun acceleration voltage +50, +100, and +300 V (Other conditions: O_2 flow rate; 18 sccm, the rf power; 300 W, V_e; −100 V).

Acceleration grid voltage (V)	Deposition rates (nm/s)	Resistivity (Ω·cm)
+50	0.10	8.5×10^{-4}
+100	0.12	8.1×10^{-4}
+300	0.16	5.1×10^{-4}

beam is varied from +50 to +300 V. This is because the distance between the ion gun and the substrate is far enough to cause the loss of oxygen ions at low energy. The distance and working pressure in this study were approximately 60 cm and 2×10^{-4} Torr, respectively. In general, the mean free path in the range of 10^{-4} Torr is known to be approximately 50 cm. Therefore, the optimum conditions with the lowest resistance should be different at each oxygen beam energy. Table I shows the oxygen ion gun acceleration voltage, the IO deposition rate, and the resistivity of the IO film deposited at each V_a. As shown in the table, the optimized resistivity decreased from 8.5×10^{-4} to 5.1×10^{-4} Ω·cm with increasing V_a of the oxygen ion gun from +50 to +300 V, while the IO deposition rate increased from 0.10 to 0.16 nm/s.

The TEOLED device structure requires a high aperture ratio, which can be obtained using a highly reflective and low resistive anode in addition to a highly transmittable and low resistive cathode. Figure 2(a) shows the reflectance spectrum of the Ag (100 nm)/ITO (125 nm) anode layer, and Fig. 2(b) shows the transmittance spectrum of IO deposited at various V_a used in this study. In addition, the inset of Fig. 2(b) shows the transmittance spectrum of Al/Au. Meanwhile, in the microcavity structures in TEOLED consisting of glass/Ag (100 nm)/ITO (x nm)/2-TNATA (30 nm)/NPB (15 nm)/Alq_3 (55 nm)/LiF (1 nm)/Al (2 nm)/Au (20 nm)/IO (100 nm), the EL intensities were investigated as a function of the ITO thickness. The relative EL intensity, which is the maximum luminance, of devices with a 25-, 50-, 125-, and 200-nm-thick ITO layer were 950, 2500, 5500, and 4500 (arb. units), respectively. Moreover, the TEOLED with the 125-nm-thick ITO exhibited the maximum EL output and the maximum peak of this device was 535 nm. As shown in Fig. 2(a), the Ag/ITO anode layer, where a 125-nm-thick sputtered ITO layer was used to obtain the maximum EL output, showed a reflectivity of 87% at a wavelength ranging from approximately 440 to 650 nm. For the IO cathode capping layer deposited by IBAD and the semi-transparent Al (2 nm)/Au (20 nm) buffer layer, as shown in Fig. 2(b), the transparency of the IO films ranged from 85 to 91% when the V_a was increased from +50 to +300 V, and the Al (2 nm)/Au (20 nm) buffer layer showed a transparency of 60% at a wavelength of 535 nm.

TEOLED devices consisting of glass/Ag (100 nm)/ITO (125 nm)/2-TNATA (30 nm)/NPB (15 nm)/Alq_3 (55 nm)/LiF (1 nm)/Al (2 nm)/Au (20 nm)/IO (100 nm) were fabricated using both Ag (100 nm)/ITO (125 nm) as the anode with a high reflectance and a low resistance and Al (2 nm)/Au (20 nm)/IO (100 nm) as the cathode having a high transmittance and low resistance.

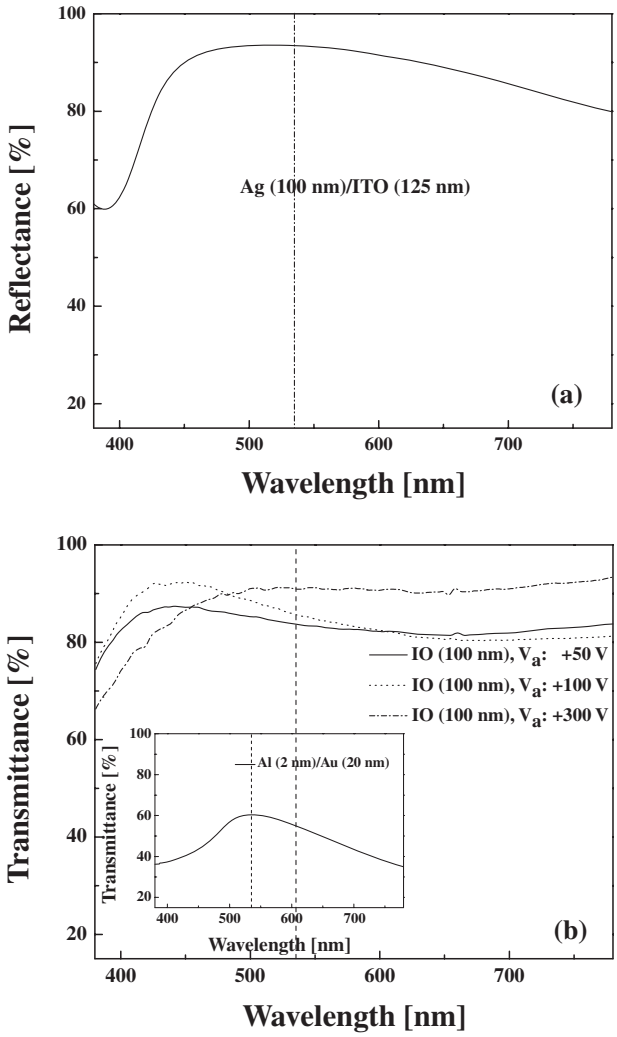

Fig. 2. (a) Reflectance spectrum of the multilayer anode consisting of Ag (100 nm)/ITO (125 nm). (b) The curves show the transmittance spectra for the 100-nm-thick IO films deposited using the IBAD at the V_a of +50 (dash line), +100 (dot line), and +300 V (dot dash line), respectively. During IBAD deposition, the O_2 flow rate, the rf power, and V_e were maintained at 18 sccm, 300 W, and −100 V, respectively. The inset shows the transmittance spectrum for Al (2 nm)/Au (20 nm) consisting of the multilayer cathode.

Figure 3(a) shows the current density–voltage–luminance characteristics of the TEOLED devices measured as a function of the forward bias voltage to the device with the IO deposited at various V_a. Indeed, the thickness of Au in the Al/Au cathode buffer layer needs to be decreased further in order to increase the transmittance of the device. However, the devices were unstable when the thickness of Au was decreased to 10 or 15 nm, and were inoperable possibly due to the damage when a 100-nm thick IO layer was deposited on the buffer layers. Therefore, an Al (2 nm)/Au (20 nm) bilayer was used as the cathode buffer layer in this experiment. When the V_a for the IO deposition was +300 V, the device was also inoperable even with Al (2 nm)/Au (20 nm), which is possibly due to physical damage to the device. Therefore, in Fig. 3(a), the device characteristics for a low V_a of +50 and +100 V are shown in addition to the characteristics of the device before the deposition of the IO layer (reference). Figure 3(a) shows the turn-on voltage of the devices, which is defined as the voltage needed to deliver a luminance of

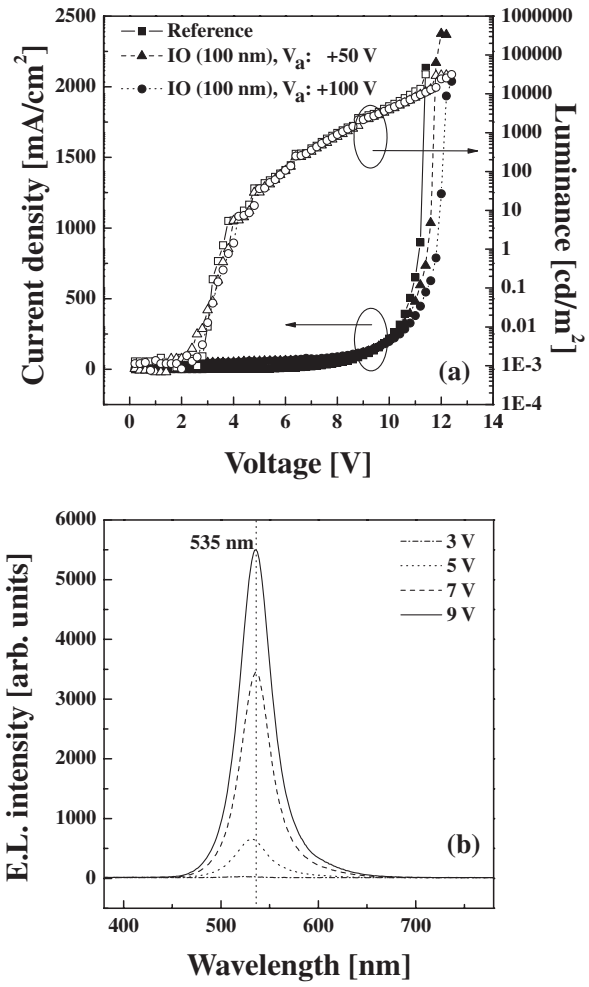

Fig. 3. (a) Curves show the current density–voltage–luminance characteristics when V_a is +50 (triangle symbol) and +100 V (circle symbol). The reference device (square symbol) shows the same structure without an IO capping cathode layer. (b) The curve shows the EL spectrum of the TEOLED with a capping IO cathode layer deposited by IBAD at a V_a of +50 V. During IBAD deposition, the O_2 flow rate, the rf power, and V_e were maintained at 18 sccm, 300 W, and −100 V, respectively.

1 cd/m^2. The turn-on voltage of the reference device was 3.6 V, and the voltage was increased slightly to 3.8 and 4.0 V by depositing IO with a V_a of +50 and +100 V, respectively. In Fig. 3(a), the maximum luminance (L_{max}) of the devices was similar at approximately 32,000 cd/m^2. However, the voltages at the maximum luminance were also slightly different. The reference device showed a maximum luminance at 11.4 V while the devices with IO deposited at +50 and +100 V_a showed a maximum luminance at 12.2 and 12.4 V, respectively. Indeed, the increase in the turn-on voltage and the increase in the voltage at the maximum luminance by depositing IO with V_a from +50 to +100 V were not significant. Therefore, it is believed that the devices were not damaged by the deposition of IO using oxygen IBAD with a $V_a < +100$ V.

Figure 3(b) shows the EL spectrum in the TEOLED between 3 and 9 V, which have an IO thin film deposited at V_a of +50 V. As shown in Fig. 3(b), the maximum EL wavelength of the device was 535 nm, and the maximum EL wavelength was not change significantly with increasing operation voltage from 3 to 9 V. The corresponding Commission Internationale de L'Eclairage (CIE) chromaticity coordinate were (0.322 – 0.300, 0.528 – 0.647) at the range of the applied voltage.

Organic materials are generally damaged by the energy[10] required to break C–C (3.73 eV), C–O (3.52 eV), C=C (6.21 eV), and C–H bonds (4.45 eV) in the organic layers such Alq_3, NPB, and 2-TNATA. All organic layers were damaged at an energy > 7 eV. During TCO deposition using the IBAD system, organic layers could be damaged by effect of bombardment by energetic particles such as ions, the radiation effect of strong light in the ultraviolet range, heating the organic layers above the glass transition temperature, the charging effect on the organic layers, etc. In particular, the oxygen ion energy generated from the oxygen ion gun is proportional to the acceleration voltage. Although a large V_a between +50 and +300 V was used, the TEOLED was not damaged significantly at a V_a of below +100 V. This can be explained by the prevention of organic damage from energetic oxygen ion species by introducing an Al (2 nm)/Au (20 nm) cathode buffer layer during IO deposition. Therefore, the stable driving performance of the TEOLED with an Al (2 nm)/Au (20 nm) layer can be improved by reducing the interaction between the organic layers and the oxygen plasma.

4. Conclusions

A transparent conducting IO film was deposited on TEOLED devices consisting of glass/Ag (100 nm)/ITO (100 nm)/2-TNATA (30 nm)/NPB (15 nm)/Alq_3 (55 nm)/LiF (1 nm)/Al (2 nm)/Au (20 nm) using an oxygen IBAD process to reduce the level of damage to the organic layers of the TEOLED device. The optical and electrical characteristics of the IO thin film deposited using oxygen IBAD improved with increasing oxygen ion energy during deposition. Meanwhile, the application of a capping IO thin film to the TEOLED device as a cathode layer damaged the device when the V_a was >+300 V. However, there was no significant damage to the TEOLED with a cathode buffer layer of Al (2 nm)/Au (20 nm) when the IO film was deposited at a $V_a < +100$ V. IO films with a resistivity of 8.5×10^{-4} Ω·cm and a transmittance of 85% were deposited at a V_a of +50 V, and the TEOLED device with these IO layers showed a high luminance of approximately 32,000 cd/m^2 at 12.2 V.

Acknowledgments

This work was supported by the National Research Laboratory Program (NRL) by the Korea Ministry of Science and Technology and the National Program for Tera-Level Nanodevices of the Korea Ministry of Science and Technology as a 21st Century Frontier Program.

1) C. W. Tang and S. A. VanSlyke: Appl. Phys. Lett. **51** (1987) 913.
2) F. Li, H. Tang, J. Anderegg and J. Shinar: Appl. Phys. Lett. **70** (1997) 1233.
3) J. H. Burroughes, D. D. C. Bradley, A. R. Brown, R. N. Marks, K. Mackay, R. H. Friend, P. L. Burns and A. B. Holmes: Nature (London) **347** (1990) 539.
4) G. Gu, G. Parthasarathy, P. E. Burrows, P. Tian, I. G. Hill, A. Khan and S. R. Forrest: J. Appl. Phys. **86** (1999) 4067.
5) G. Parthasarathy, C. Adachi, P. E. Burrows and S. R. Forrest: Appl. Phys. Lett. **76** (2000) 2128.

6) T. Minami: MRS Bull. **25** (2000) 38.
7) A. J. Freeman, K. R. Poeppelmeier, T. O. Mason, R. P. H. Chang and T. J. Marks: MRS Bull. **25** (2000) 45.
8) K. L. Chopra, S. Major and D. K. Pandya: Thin Solid Films **102** (1983) 1.
9) T. H. Chen, Y. Liou, T. J. Wu and J. Y. Chen: Appl. Phys. Lett. **85** (2004) 2092.
10) H. K. Kim, D. G. Kim, K. S. Lee, M. S. Huh, S. H. Jeong, K. I. Kim and T. Y. Seong: Appl. Phys. Lett. **86** (2005) 183503.
11) H. Suzuki and M. Hikita: Appl. Phys. Lett. **68** (1996) 2276.
12) D. M. Mattox: J. Vac. Sci. Technol. A **7** (1989) 1105.
13) L. S. Hung, C. W. Tang, M. G. Mason, P. Raychandhuri and J. Madathil: Appl. Phys. Lett. **78** (2001) 544.
14) J. F. Moulder, W. F. Stickle, P. E. Sobol and K. D. Bomben: *Handbook of X-ray Photoelectron Spectroscopy* (Physical Electronics, Minnesota, 1995) pp. 125 and 224.
15) J. W. Bae, H. C. Lee and G. Y. Yeom: J. Korean Phys. Soc. **47** (2005) 889.